




# Osteopetrosis-Associated Transmembrane Protein 1 Recruits RNA Exosome To Restrict Hepatitis B Virus Replication

Chunqiang Ma,<sup>a</sup> Wei Xu,<sup>a</sup> Qingyu Yang,<sup>a</sup> Weiyong Liu,<sup>a</sup> Qi Xiang,<sup>a</sup> Junbo Chen,<sup>a</sup> Qi Zhang,<sup>a</sup> Yingle Liu,<sup>a,b</sup> Kailang Wu,<sup>a</sup>  
 Jianguo Wu<sup>a,b</sup>

<sup>a</sup>State Key Laboratory of Virology, College of Life Sciences, Wuhan University, Wuhan, China

<sup>b</sup>Guangdong Key Laboratory of Virology, Institute of Medical Microbiology, Jinan University, Guangzhou, China

**ABSTRACT** Hepatitis B virus (HBV) chronically infects approximately 350 million people worldwide, and 600,000 deaths are caused by HBV-related hepatic failure, liver cirrhosis, and hepatocellular carcinoma annually. It is important to reveal the mechanism underlying the regulation of HBV replication. This study demonstrated that osteopetrosis-associated transmembrane protein 1 (Ostm1) plays an inhibitory role in HBV replication. Ostm1 represses the levels of HBeAg and HBsAg proteins, HBV 3.5-kb and 2.4/2.1-kb RNAs, and core-associated DNA in HepG2, Huh7, and NTCP-HepG2 cells. Notably, Ostm1 has no direct effect on the activity of HBV promoters or the transcription of HBV RNAs; instead, Ostm1 binds to HBV RNA to facilitate RNA decay. Detailed studies further demonstrated that Ostm1 binds to and recruits the RNA exosome complex to promote the degradation of HBV RNAs, and knockdown of the RNA exosome component exonuclease 3 (Exosc3) leads to the elimination of Ostm1-mediated repression of HBV replication. Mutant analyses revealed that the N-terminal domain, the transmembrane domain, and the C-terminal domain are responsible for the repression of HBV replication, and the C-terminal domain is required for interaction with the RNA exosome complex. Moreover, Ostm1 production is not regulated by interferon- $\alpha$  (IFN- $\alpha$ ) or IFN- $\gamma$ , and the expression of IFN signaling components is not affected by Ostm1, suggesting that Ostm1 anti-HBV activity is independent of the IFN signaling pathway. In conclusion, this study revealed a distinct mechanism underlying the repression of HBV replication, in which Ostm1 binds to HBV RNA and recruits RNA exosomes to degrade viral RNA, thereby restricting HBV replication.

**IMPORTANCE** Hepatitis B virus (HBV) is a human pathogen infecting the liver to cause a variety of diseases ranging from acute hepatitis to advanced liver diseases, fulminate hepatitis, liver cirrhosis, and hepatocellular carcinoma, thereby causing a major health problem worldwide. In this study, we demonstrated that Ostm1 plays an inhibitory role in HBV protein production, RNA expression, and DNA replication. However, Ostm1 has no effect on the activities of the four HBV promoters; instead, it binds to HBV RNA and recruits RNA exosomes to promote HBV RNA degradation. We further demonstrated that the anti-HBV activity of Ostm1 is independent of the interferon signaling pathway. In conclusion, this study reveals a distinct mechanism underlying the repression of HBV replication and suggests that Ostm1 is a potential therapeutic agent for HBV infection.

**KEYWORDS** hepatitis B virus, HBV, osteopetrosis-associated transmembrane protein 1, Ostm1, RNA exosome complex, hepatitis B e antigen, HbeAg, hepatitis B surface antigen, HbsAg, exonuclease, EXO, HBV RNA degradation, HBV core-associated DNA, HBV 3.5-kb and 2.4/2.1-kb RNAs

**Citation** Ma C, Xu W, Yang Q, Liu W, Xiang Q, Chen J, Zhang Q, Liu Y, Wu K, Wu J. 2020. Osteopetrosis-associated transmembrane protein 1 recruits RNA exosome to restrict hepatitis B virus replication. *J Virol* 94:e01800-19. <https://doi.org/10.1128/JVI.01800-19>.

**Editor** J.-H. James Ou, University of Southern California

**Copyright** © 2020 American Society for Microbiology. All Rights Reserved.

Address correspondence to Kailang Wu, wukailang@whu.edu.cn, or Jianguo Wu, jwu@whu.edu.cn.

**Received** 18 October 2019

**Accepted** 22 January 2020

**Accepted manuscript posted online** 18 March 2020

**Published** 18 May 2020

Hepatitis B virus (HBV), a major human pathogen, chronically infects more than 350 million individuals worldwide and causes a variety of liver diseases ranging from acute hepatitis (AH), chronic hepatitis B (CHB), and fulminant hepatitis (FH) to liver cirrhosis (LC) and hepatocellular carcinoma (HCC) (1). The HBV genome comprises a partially double-stranded 3.2-kb relaxed circular DNA (rcDNA) organized into four open reading frames (ORFs). The host DNA repair pathway converts the rcDNA to the covalently closed circular DNA (cccDNA) in the cell nucleus. The cccDNA serves as the transcription template of HBV mRNAs. In the cytoplasm, the transcripts are translated into virus proteins, and the pregenomic RNA (pgRNA) is reverse transcribed to viral DNA by the viral polymerase. The newly formed rcDNA encapsidated by core protein is enveloped by surface proteins and secreted as virions (2).

Osteopetrosis-associated transmembrane protein 1 (Ostm1) was identified in a spontaneous gray-lethal mutant in mice (3–5). Ostm1 is highly conserved, and the human Ostm1 gene encodes a 334-amino acid protein that is 83% homologous to the mouse protein. Ostm1 expression is prevalent in brain, spleen, kidney, osteoclasts, and melanocytes but is expressed at lower levels in thymus, liver, testis, heart, and primary osteoclasts (3). Ostm1 is a type I transmembrane protein that localizes to intracellular vesicles (mainly endoplasmic reticulum [ER], endosomes, and lysosomes). Ostm1 serves as a  $\beta$ -subunit of chloride channel protein-7 (CIC-7) to support bone restoration and lysosomal function in osteoclasts (6), interacts with RGS-GAIP to degrade the heterotrimeric G protein subunit ( $G\alpha i3$ ) (7), regulates  $\beta$ -catenin/Lef1 interaction to activate Wnt/ $\beta$ -catenin signaling (8), functions as an antiadipogenic factor (9), and forms a cytosolic scaffolding multiprotein complex with kinesin 5B (10).

Mammalian cells have evolved a highly organized and complex mRNA degradation system (11). When a typical cellular mRNA is targeted for decay, it initially undergoes deadenylation-removal of the 3' poly(A) tail by poly(A)-specific RNase (PARN), the CCR4-NOT complex, or the Pan2-Pan3 complex (11). The mRNA is subject to processive exonucleolytic degradation in either the 3' to 5' (3'-5') direction by the RNA exosome, or it is marked by the LSM1-7/Pat1 complex for decapping by Dcp1/2 and degraded in the 5'-3' direction by Xrn1 (12, 13). The RNA exosome complex degrades a vast array of different RNA substrates (rRNAs, small nuclear RNAs, and tRNAs) or catalyzes RNA 3' to 5' processing in the nucleus and cytoplasm (14). The nuclear exosome also functions in the surveillance system, in which the transcripts with defects generated in the RNA processing and exporting pathways are degraded, and the cytoplasmic exosome plays a key role in degrading aberrant or unused intermediate mRNAs and AU-rich element (ARE)-containing mRNAs (13, 14). The human RNA exosome consists of a nine-subunit core (exonucleases 1 to 9 [EXOS1 to 9]) and cofactors (nuclear matrix protein C1D and Mapp6). The barrel-shaped nine-subunit core is catalytically inactive and includes six RNase Pleckstrin homology (PH)-like domain-containing proteins (EXOS4 to 9). The ring is capped by a ring of three proteins that are collectively termed the S1/KH cap (15). Catalytic subunits of the RNA exosome include EXOS10 and at least an isoform of Dis3. Dis3 and Dis3L include an active site that has a processive  $Mg^{2+}$ -dependent hydrolytic 3'-5' exoribonuclease activity (16, 17). The nuclear subunit EXOS10 includes a single active site that catalyzes  $Mg^{2+}$ -dependent distributive 3'-5' hydrolytic exoribonuclease activity (18). The host RNA-decay machineries have been implicated in the host defense against viral infection. Zinc-finger antiviral protein, AID, MyD88, and Prdx1 can inhibit HBV replication by degrading HBV mRNAs dependent on the RNA exosome (19–22). The RNA exosome complex regulates the stability of the HBV X-mRNA transcript in a non-stop-mediated (NSD) RNA quality control mechanism (23).

This study demonstrates that Ostm1 plays an inhibitory role in HBeAg and HBsAg expression, HBV RNA production, and core-associated DNA replication. Notably, Ostm1 has no effect on the activities of the four HBV promoters. Instead, Ostm1 binds to HBV RNA and recruits the RNA exosome complex to promote the degradation of the viral RNAs. Moreover, the anti-HBV activity of Ostm1 is independent of the IFN signaling pathway. Therefore, this study revealed a distinct mechanism by which Ostm1 binds to

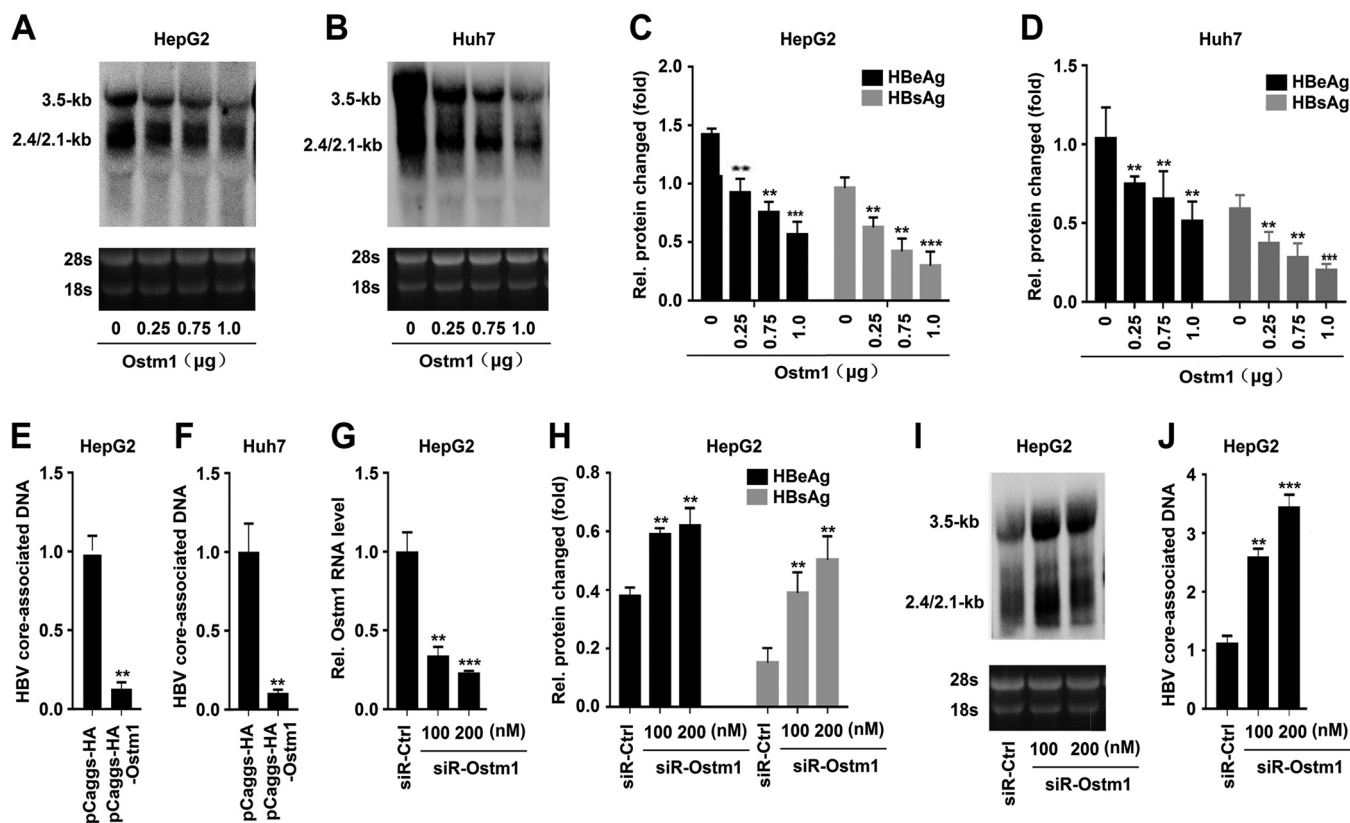


**FIG 1** Ostm1 represses HBV replication in hepatoma cell lines. (A to F) HepG2 and Huh7 cells were cotransfected with different concentrations of pCaggs-Ostm1 and pBlue-HBV 1.3 for 48 h (A to D) or 96 h (E to F). (G to J) HepG2 and Huh7 cells were cotransfected with different concentrations of siR-Ostm1 and pBlue-HBV 1.3 for 48 h (G, H, and I) or 96 h (J). (A, B, and I) Northern blot analysis of HBV transcripts. The rRNAs (18s and 28s) were used as a loading control. (C, D, and H) Secreted HBsAg and HBeAg in cell culture supernatants were detected using an ELISA kit. (E, F, and J) HBV core-associated DNAs were extracted and measured using qRT-PCR. (J) The level of Ostm1 mRNA was measured with qRT-PCR. \*,  $P < 0.05$ ; \*\*,  $P < 0.01$ ; \*\*\*,  $P < 0.001$ .

HBV RNA and recruits the RNA exosome to degrade the viral RNAs, thereby restricting HBV replication.

## RESULTS

**Ostm1 represses HBV replication in hepatoma cell lines.** Ostm1, a type I transmembrane protein, cooperates with chloride channel 7 (CIC7) to support the bone development or osteopetrosis (3, 6). However, the role of Ostm1 in the regulation of HBV replication has not been reported. Here, we initially investigated the effect of Ostm1 on the regulation of HBV replication in HepG2 cells and Huh7 cells transfected with pBlue-HBV1.3 and Ostm1 expression plasmid (pCaggs-Ostm1) at different concentrations. The results revealed that the levels of HBV 3.5-kb and 2.4/2.1-kb RNAs (Fig. 1A and B) as well as the abundances of the secreted viral proteins hepatitis B e antigen (HBeAg) and hepatitis B surface antigen (HBsAg) (Fig. 1C and D) were significantly attenuated by Ostm1 in dose-dependent manners in HepG2 cells (Fig. 1A and C) and Huh7 cells (Fig. 1B and D). Similarly, HBV core-associated DNA was notably repressed by Ostm1 in HepG2 and Huh7 cells (Fig. 1E and F). These results showed that overexpression of Ostm1 attenuates HBV replication. To further illustrate the role of endogenous Ostm1 in the regulation of HBV replication, the Ostm1 expression in HepG2 cells was knocked down by a small interfering RNA (siRNA) specifically targeting Ostm1 (siR-Ostm1). The mRNA level of endogenous Ostm1 was markedly decreased in HepG2 cells transfected with siR-Ostm1 (Fig. 1G), indicating that siR-Ostm1 is effective in the cells. The levels of HBV-secreted HBeAg and HBsAg proteins (Fig. 1H), 3.5-kb and 2.4/2.1-kb RNAs (Fig. 1I), and HBV core-associated DNA (Fig. 1J) were enhanced by siR-Ostm1 in HepG2 cells, suggesting that knockdown of Ostm1 promotes HBV repli-

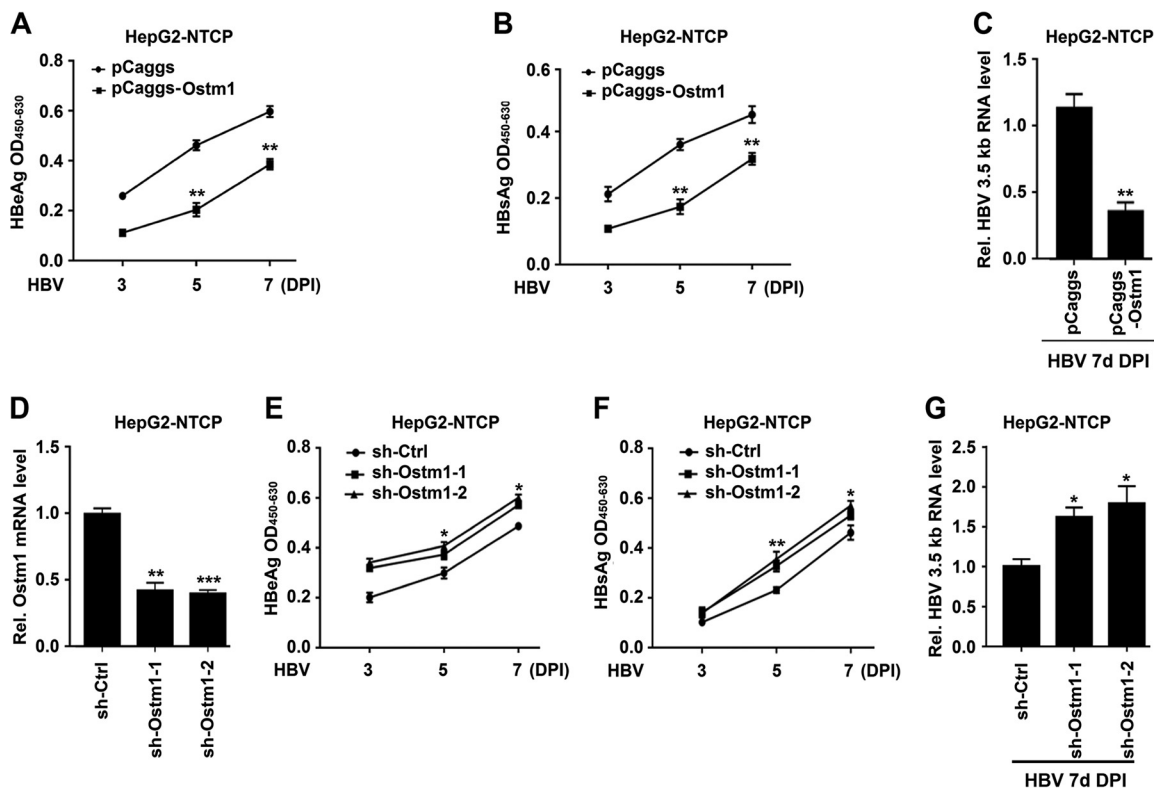


**FIG 2** Ostm1 represses HBV infection in the HepG2-NTCP infection system. (A to G) HepG2-NTCP cells were independently cotransfected with Ostm1 (A to C) and sh-Ctrl or sh-Ostm1 (D to G) for 24 h and then inoculated with HBV for different times, as indicated, in the presence of 4% PEG 8000. (A, B, E, and F) The levels of HBsAg and HBeAg in the supernatants were determined using an ELISA kit. (C and G) Total cellular RNAs were extracted from the cells, and HBV 3.5-kb RNA was measured using qRT-PCR. (D) Ostm1 mRNA was quantified using qRT-PCR. \*,  $P < 0.05$ ; \*\*,  $P < 0.01$ ; \*\*\*,  $P < 0.001$ .

cation. Collectively, these results showed that Ostm1 plays an inhibitory role in HBV replication in HepG2 and Huh7 cells.

**Ostm1 represses HBV infection in the HepG2-NTCP infection system.** The effect of Ostm1 on HBV infection was further investigated in the HepG2-NTCP infection system as established previously (24, 25). Initially, HepG2-NTCP cells were transfected with pCaggs-Ostm1 and control vector for 24 h and infected with HBV by inoculation with supernatants of HepaAD38 cells. In HBV-infected HepG2-NTCP cells, the levels of secreted HBeAg (Fig. 2A), secreted HBsAg (Fig. 2B), and HBV 3.5-kb RNA (Fig. 2C) were repressed by Ostm1, indicating that overexpression of Ostm1 attenuates HBV infection. Additionally, the effect of endogenous Ostm1 on HBV replication was evaluated by two short hairpin RNA-targeting Ostm1s (sh-Ostm1-1 and sh-Ostm1-2). The reverse transcription-quantitative PCR (qRT-PCR) results showed that Ostm1 was significantly attenuated by sh-Ostm1-1 and sh-Ostm1-2 (Fig. 2D), indicating that the shRNAs are effective in HepG2-NTCP cells. The cells were transfected with sh-Ostm1-1 or sh-Ostm1-2 and then infected with HBV by inoculation with supernatants of HepaAD38 cells. The results showed that secreted HBeAg (Fig. 2E), secreted HBsAg (Fig. 2F), and HBV 3.5-kb RNA (Fig. 2G) were upregulated in the presence of sh-Ostm1-1 or sh-Ostm1-2, suggesting that knockdown of Ostm1 promotes HBV infection. Taken together, this evidence demonstrated that Ostm1 represses HBV infection in the HepG2-NTCP infection system.

**Ostm1 attenuates HBV RNAs via posttranscription regulation.** To reveal the mechanism underlying the repression of HBV replication mediated by Ostm1, the effects of Ostm1 on the activities of four HBV promoters were investigated with luciferase-based reporter assays. HepG2 cells were cotransfected with pCaggs-Ostm1, and each of the generated reporters was driven by EnhI/Xp, EnhII/Cp, SP1, and SP2

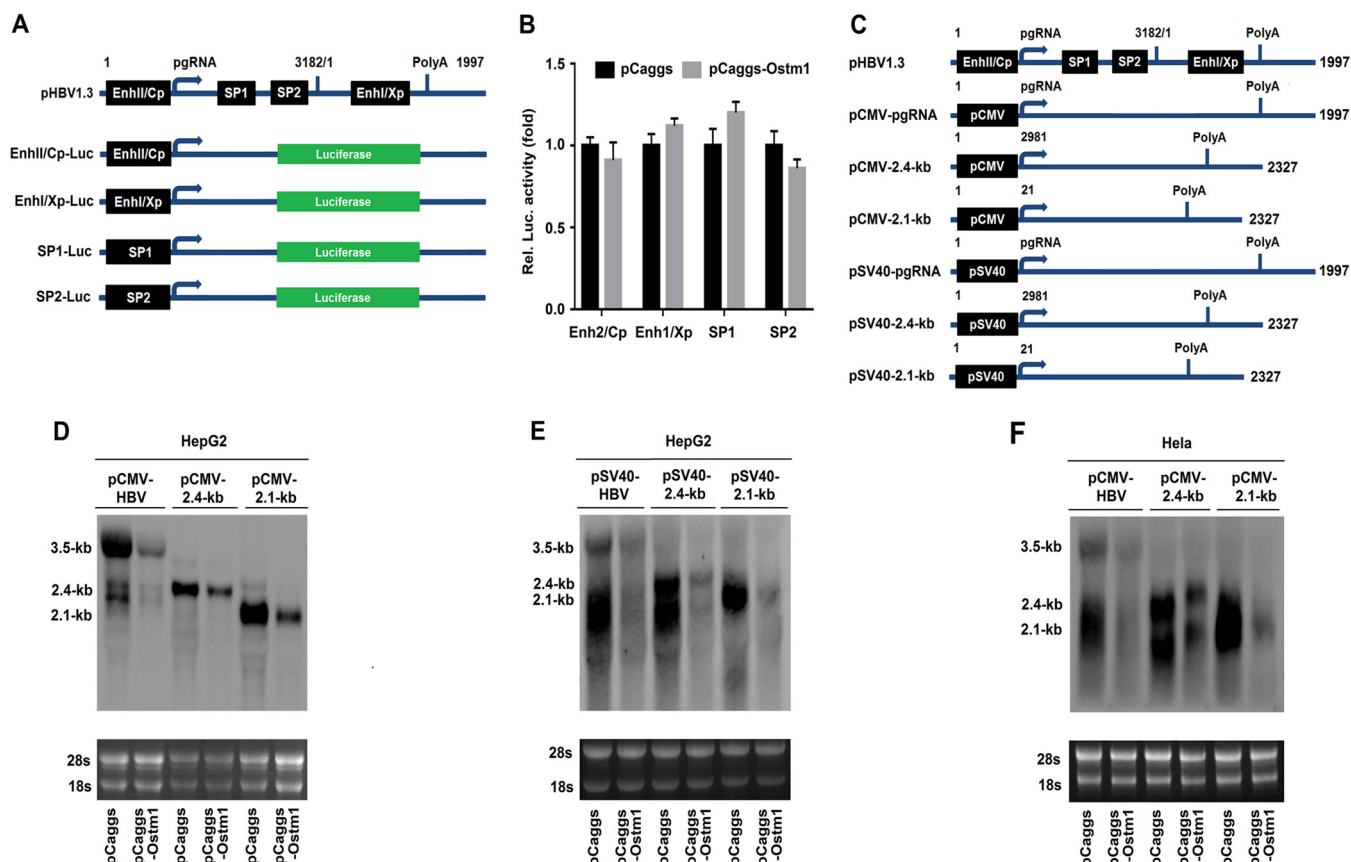


**FIG 3** Ostm1 attenuates HBV RNAs via posttranscription regulation. (A) Schematic diagrams of reporters driven by EnhI/Xp, EnhII/Cp, SP1, and SP2 promoters. (B) HepG2 cells were separately transfected with the reporters driven by EnhI/Xp, EnhII/Cp, SP1, and SP2 promoters along with plasmid Ostm1 or control vector for 48 h. Cells were harvested, and luciferase activities were measured. (C) Schematic diagrams of transcripts under the control of the CMV or SV40 promoter. (D and E) HepG2 cells were cotransfected with the plasmids expressing HBV RNAs under the control of CMV (D) or SV40 (E) promoter and Ostm1 expression construct. (F) HeLa cells were cotransfected with the plasmids expressing HBV RNAs under the control of the SV40 promoter and Ostm1 expression construct. (D to F) Cells were harvested at 48 h after transfection, and the levels of transcripts were determined with Northern blotting. \*,  $P < 0.05$ ; \*\*,  $P < 0.01$ ; \*\*\*,  $P < 0.001$ .

promoters, respectively (Fig. 3A). The results unexpectedly showed that the activities of the four HBV promoters were not affected by Ostm1 (Fig. 3B). We then clarified whether the intrinsic promoters of HBV are required for the inhibition by Ostm1. Several plasmids were generated, in which HBV 3.5-kb RNA, 2.4-kb RNA, and 2.1-kb RNA were under the control of cytomegalovirus (CMV) promoter or Simian virus 40 (SV40) promoter (Fig. 3C). The results revealed that HBV 3.5-kb RNA, 2.4-kb RNA, and 2.1-kb RNA controlled by CMV promoter (Fig. 3D) or by SV40 promoter (Fig. 3E) were repressed by Ostm1 in HepG2 cells. Moreover, we determined whether the suppressive effect of Ostm1 on HBV RNAs was limited to hepatocyte-derived cell lines. Similarly, HBV 3.5-kb RNA, 2.4-kb RNA, and 2.1-kb RNA controlled by CMV promoter were significantly attenuated by Ostm1 in HeLa cells (Fig. 3F). Collectively, these results suggested that Ostm1 represses the levels of HBV 3.5-kb RNA, 2.4-kb RNA, and 2.1-kb RNA via a posttranscription mechanism.

**Ostm1 facilitates the degradation of HBV RNAs in the cytoplasm.** We speculated that Ostm1 may promote the turnover rate of HBV pgRNA. pTRE2-HBV was constructed, in which the HBV pgRNA is transcribed from a tetracycline-controlled promoter. HepG2 cells were transfected with pTRE2-HBV and pCaggs-Ostm1 for 36 h and then treated with doxycycline (DOX) for 0, 3, 6, and 9 h to turn off HBV RNA transcription (Fig. 4A, top). Northern blot analysis revealed that HBV 3.5-kb RNA, 2.4-kb RNA, and 2.1-kb RNA were attenuated by DOX in time-dependent manners (Fig. 4A, bottom). Notably, the levels of HBV RNAs were significantly lower in Ostm1-transfected cells than in the

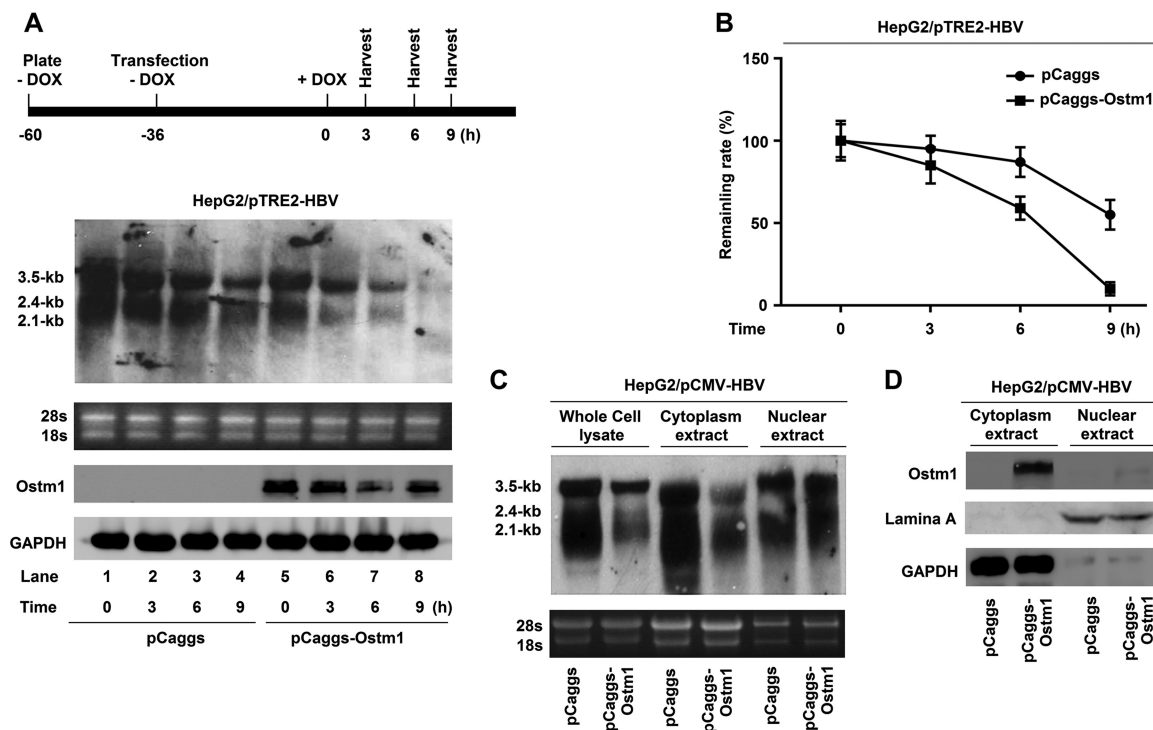


**FIG 4** Ostm1 facilitates the degradation of HBV RNAs in the cytoplasm. (A) HepG2 cells were cotransfected with pTet-Off, pTRE2-HBV, and Ostm1 expression vector for 36 h. Doxycycline hyclate (DOX) was added to the culture medium to turn off the pgRNA transcription. Cells were harvested 0, 3, 6, and 9 h after DOX addition. Total RNA was extracted and analyzed for HBV transcripts. Expression of Ostm1 was detected with Western blotting. (B) Kinetic analysis of HBV RNA decay in the absence or presence of Ostm1 overexpression. The relative levels of HBV RNAs from each sample were expressed as the percentage of the RNA signals from the corresponding sample at time point 0 h. (C and D) Subcellular distribution and antiviral activity of Ostm1. HepG2 cells were cotransfected with plasmid pCMV-HBV and Ostm1 expression vector for 48 h. Cells were harvested. Cell fractionations for RNA and protein analysis were performed as described in Materials and Methods. (C) Total cellular RNA and cytoplasmic and nuclear RNA were isolated and subjected to Northern blot analysis of HBV RNAs. (D) Subcellular distribution of Ostm1 was revealed using Western blotting; LaminaA and GAPDH were used to confirm the purity of nuclear and cytoplasmic fraction.

control cells (Fig. 4A, lanes 5 to 8 versus lanes 1 to 4). Moreover, the decay rate of HBV RNAs was significantly higher in Ostm1-transfected cells than in the control cells (Fig. 4B). These results indicated that Ostm1 facilitates HBV RNA degradation.

As Ostm1 localizes to intracellular vesicles, mainly endoplasmic reticulum, endosomes, and lysosomes (6, 10), we determined the subcellular distribution and antiviral activity of Ostm1. HepG2 cells were cotransfected with pCMV-HBV and pCaggs-Ostm1 for 48 h. Northern blot analysis revealed that HBV 3.5-kb RNA, 2.4-kb RNA, and 2.1-kb RNA were significantly attenuated by Ostm1 in the whole-cell lysates and cytoplasm extracts, whereas they were relatively unaffected by Ostm1 in the nuclear extracts (Fig. 4C). Western blot analysis clearly showed that Ostm1 was highly expressed in the cytoplasm extracts, whereas it was not detected in the nuclear extracts (Fig. 4D). These results indicated that Ostm1 is mainly distributed in the cytoplasm to promote the degradation of HBV RNAs.

**Ostm1 binds to the sequences 837 to 1065 and 1598 to 1796 of HBV RNA to facilitate RNA decay.** We next attempted to map the sequences of HBV RNAs required for Ostm1-mediated degradation of HBV RNAs. A series of HBV genomic DNA deletion mutants was generated, and they were then individually inserted into the multiple-cloning site of pcDNA3.1/ $\beta$ -gal (Fig. 5A). In HepG2 cells, the  $\beta$ -gal activities derived from pcDNA3.1/ $\beta$ -gal-HBV (1812 to 3182/1 to 1997), pcDNA3.1/ $\beta$ -gal-HBV (22 to 1997), pcDNA3.1/ $\beta$ -gal-HBV (22 to 1066), pcDNA3.1/ $\beta$ -gal-HBV (937 to 1797), and pcDNA3.1/ $\beta$ -gal-HBV (1066 to 1997) were significantly reduced by Ostm1, whereas the  $\beta$ -gal activities derived from pcDNA3.1/ $\beta$ -gal, pcDNA3.1/ $\beta$ -gal-HBV (1812 to 21), pcDNA3.1/ $\beta$ -gal-HBV (22 to 836), pcDNA3.1/ $\beta$ -gal-HBV (22 to 936), pcDNA3.1/ $\beta$ -gal-HBV (937 to

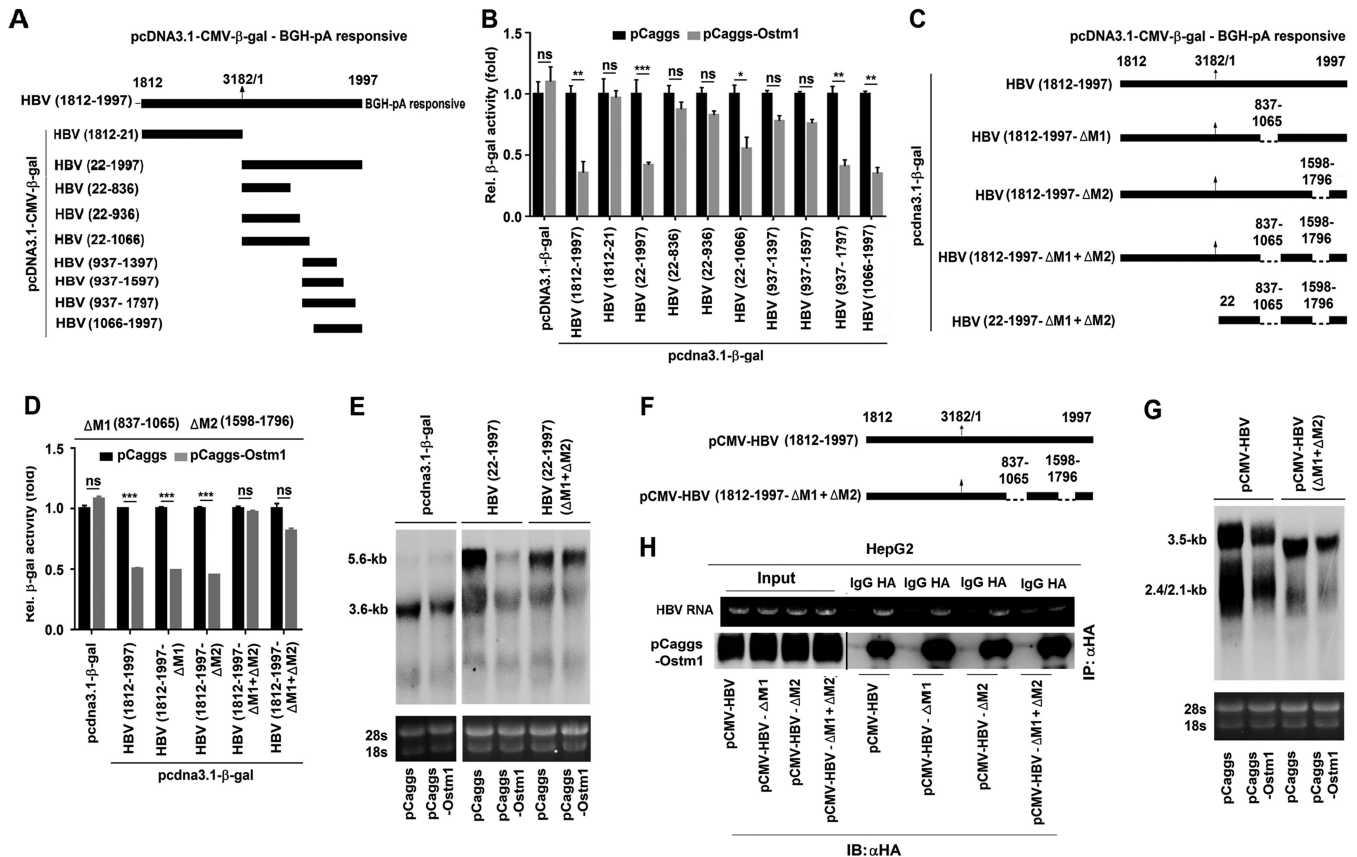


**FIG 5** Ostm1 binds to the sequences 837 to 1065 and 1598 to 1796 of HBV RNA to facilitate the viral RNA decay. (A) Schematic diagrams of the truncation mutants of HBV pregenomic RNA. The numbers indicate the HBV DNA sequence with 1 at the unique EcoRI site in the HBV genome. (B) HepG2 cells were transfected with fusion constructs (containing HBV DNA or the truncation mutants of HBV DNA) and plasmid Ostm1 or control vector for 48 h, and the  $\beta$ -gal activity was then assessed. (C) Schematic diagrams of the deletion mutants of HBV pregenomic RNA. The numbers indicate the HBV DNA sequence with 1 at the unique EcoRI site in the HBV genome. (D and E) HepG2 cells were transfected with the deletion mutant of  $\beta$ -gal-HBV (1812 to 3182/1 to 1997) and  $\beta$ -gal-HBV (22 to 1997) together with plasmid Ostm1 or control vector for 48 h. The  $\beta$ -gal activity was then assessed (D) and levels of  $\beta$ -gal mRNA were determined with Northern blot analysis (E). (F) Schematic diagrams of the truncation mutants of HBV pregenomic RNA. (G) HepG2 cells were transfected with the deletion mutant of pCMV-HBV (1812 to 3182/1 to 1997) together with plasmid Ostm1 or control vector for 48 h, and levels of HBV mRNA were determined with Northern blot analysis. (H) To determine RNA coprecipitation with the Ostm1, HepG2 cells were cotransfected with pCaggs-ostm1 and pCMV-HBV, pCMV-HBV- $\Delta$ M1, pCMV-HBV- $\Delta$ M2, and pCMV-HBV- $\Delta$ M1+ $\Delta$ M2 for 48 h. IP using anti-HA antibody was performed; complex of HA-Ostm1 was then eluted using free HA peptides, and the eluted RNA was analyzed using RT-PCR. Western blotting was used to check the results of IP. \*,  $P < 0.05$ ; \*\*,  $P < 0.01$ ; \*\*\*,  $P < 0.001$ .

1397), and pcDNA3.1/ $\beta$ -gal-HBV (937 to 1597) were relatively unaffected by Ostm1 (Fig. 5B). These results suggested that the two nucleotide regions HBV (837 to 1065) and (1598 to 1796) are required for Ostm1-mediated degradation of HBV RNA.

Deletion mutants of the two sequences in the context of pcDNA3.1/ $\beta$ -gal-HBV (1812 to 3182/1 to 1997) and pcDNA3.1/ $\beta$ -gal-HBV (22 to 1997) were then generated (Fig. 5C). The level of  $\beta$ -gal activities derived by pcDNA3.1/ $\beta$ -gal-HBV (1812 to 1997), pcDNA3.1/ $\beta$ -gal-HBV (1812 to 1997- $\Delta$ M1), and pcDNA3.1/ $\beta$ -gal-HBV (1812 to 1997- $\Delta$ M2) was significantly repressed by Ostm1, whereas the  $\beta$ -gal activities derived by pcDNA3.1/ $\beta$ -gal, the double deletion mutant pcDNA3.1/ $\beta$ -gal-HBV (1812 to 1997- $\Delta$ M1+ $\Delta$ M2), and pcDNA3.1/ $\beta$ -gal-HBV (22 to 1997- $\Delta$ M1+ $\Delta$ M2) were not affected by Ostm1 (Fig. 5D). Similarly, the level of  $\beta$ -gal mRNA derived by pcDNA3.1/ $\beta$ -gal-HBV (22 to 1997) was significantly reduced by Ostm1, whereas the level of  $\beta$ -gal mRNA derived by pcDNA3.1/ $\beta$ -gal or pcDNA3.1/ $\beta$ -gal-HBV (22 to 1997- $\Delta$ M1+ $\Delta$ M2) was slightly reduced by Ostm1 (Fig. 5E). Additionally, to exclude the influence of the  $\beta$ -gal RNA sequence on the response of the deletion mutant to Ostm1, we constructed and analyzed pCMV-HBV ( $\Delta$ M1+ $\Delta$ M2), in which HBV (837 to 1065) and (1598 to 1796) were deleted in the context of pCMV-HBV (Fig. 5F). Northern blot analysis revealed that HBV RNAs transcribed from pCMV-HBV were largely attenuated by Ostm1, whereas HBV RNAs trans-

scribed from pCMV-HBV ( $\Delta M1 + \Delta M2$ ) were slightly reduced by Ostm1 (Fig. 5G). It is known that HBV (837 to 1065) and (1598 to 1796) sequences are common to HBV pgRNA, 2.4-kb, and 2.1-kb. Then, we determined whether Ostm1 associates with HBV transcripts. HepG2 cells were cotransfected with pCaggs-Ostm1 and pCMV-HBV, pCMV-HBV- $\Delta M1$ , pCMV-HBV- $\Delta M2$ , and pCMV-HBV- $\Delta M1 + \Delta M2$  for 48 h. Notably, RNA immunoprecipitation and RT-PCR analysis revealed that Ostm1 could bind to HBV RNA, HBV- $\Delta M1$  RNA, and pCMV-HBV- $\Delta M2$  RNA but not to HBV- $\Delta M1 + \Delta M2$  RNA. We have demonstrated that Ostm1 can decay the RNAs of HBV, HBV- $\Delta M1$ , and HBV- $\Delta M2$  but not those of HBV- $\Delta M1 + \Delta M2$  (Fig. 5H). Taken together, these results showed that Ostm1 associates with the sequences (837 to 1065) and (1598 to 1796) of HBV RNA to facilitate the viral RNA decay.

#### **The RNA exosome is involved in Ostm1-mediated degradation of HBV RNAs.**

Mammalian cells have evolved highly organized and complex mRNA degradation systems—the 5'-3' mRNA decay pathway depending on 5'-3' exoribonuclease 1 (XRN1) and the 3'-5' mRNA decay pathway relying on the RNA exosome complex (11). Exosome component 3 (Exosc3, also known as Rrp40) is noncatalytic but essential for the degradation and processing of target RNA, and the knockdown of Exosc3 severely diminishes RNA exosome function (26). Here, we determined the mRNA decay pathway required for Ostm1-induced decay of HBV RNAs. HepG2 cells were transfected with siRNA targeting Xrn1 (siR-Xrn1) or siRNA targeting Exosc3 (siR-Exosc3) together with pBlue-HBV1.3 or pCaggs-Ostm1. Xrn1 mRNA and Exosc3 mRNA were significantly attenuated by siR-Xrn1 and siR-Exosc3 (Fig. 6A), indicating that they are efficient. HBV RNAs were attenuated by Ostm1 in the presence of siR-Ctrl and siR-Xrn1, whereas they were relatively unaffected by Ostm1 in the presence of siR-Exosc3 (Fig. 6B and C), suggesting that Ostm1 reduces the level of HBV RNAs depending on the RNA exosome complex through the 3'-5' mRNA decay pathway.

Next, we investigated the correlation between Ostm1 and the RNA exosome complex. HEK293T cells were cotransfected with pFlag-Exosc3 and plasmids pGFP-Exosc2, pGFP-Exosc4, and pGFP-Exosc5 expressing other RNA exosome component proteins. The results showed that Exosc3 was coprecipitated with Exosc2, Exosc4, and Exosc5, as expected (Fig. 6D). HEK293T cells were cotransfected with pCaggs-Ostm1 and pGFP-Exosc2, pGFP-Exosc3, pGFP-Exosc4, and pGFP-Exosc5. Coimmunoprecipitation (Co-IP) results showed that Ostm1 interacted with Exosc2, Exosc3, Exosc4, and Exosc5 (Fig. 6E). Additional Co-IP results confirmed that Ostm1 could interact with Exosc2/3/4/5 in HEK293T cells cotransfected with HA-Ostm1 and Flag-Exosc2/3/4/5 (Fig. 6F). A glutathione S-transferase (GST) pulldown assay revealed that Ostm1 was pulled down by purified GST-Exosc3 (Fig. 6G). Laser scanning confocal microscopy showed that in the presence of a single protein, Ostm1 mainly localized in the cytoplasm, and Exosc3 distributed in both the cytoplasm and nuclei, whereas in the presence of both Ostm1 and Exosc3, a large proportion of the two proteins were colocalized in the cell (Fig. 6H). Collectively, the data suggested that Ostm1 interacts with Exosc3 to recruit the RNA exosome complex to HBV transcripts, leading to the downregulation of HBV RNAs.

#### **Ostm1 represses HBV replication relying on the C-terminal domain and N-terminal domain of Ostm1 in an IFN-independent manner.**

To further delineate the mechanism involved in the inhibitory effect of Ostm1 on HBV replication, we constructed five truncated mutants of Ostm1 (Ostm1- $\Delta C$ , Ostm1- $\Delta Tm$ , Ostm1- $\Delta Tm + \Delta C$ , Ostm1- $\Delta N$ , and Ostm1- $\Delta R$ ) (Fig. 7A). HepG2 cells were cotransfected with pBlue-HBV1.3 and plasmids expressing different truncated Ostm1 mutants for 48 h. Northern blot analysis results showed that the levels of HBV 3.5-kb RNA, 2.4-kb RNA, and 2.1-kb RNA were inhibited by Ostm1 and significantly attenuated by Ostm1- $\Delta R$ , whereas the level of HBV RNAs was relatively unaffected by Ostm1- $\Delta C$ , Ostm1- $\Delta Tm$ , Ostm1- $\Delta Tm + \Delta C$ , and Ostm1- $\Delta N$  (Fig. 7B). Enzyme-linked immunosorbent assay (ELISA) results indicated that the abundances of secreted HBsAg and HBeAg proteins in cell culture supernatants were significantly repressed by Ostm1 and Ostm1- $\Delta R$ , whereas they were not affected by Ostm1- $\Delta C$ , Ostm1- $\Delta Tm$ , Ostm1- $\Delta Tm + \Delta C$ , and Ostm1- $\Delta N$  (Fig. 7C). Consistently, the  $\beta$ -gal activities were significantly reduced by Ostm1 and



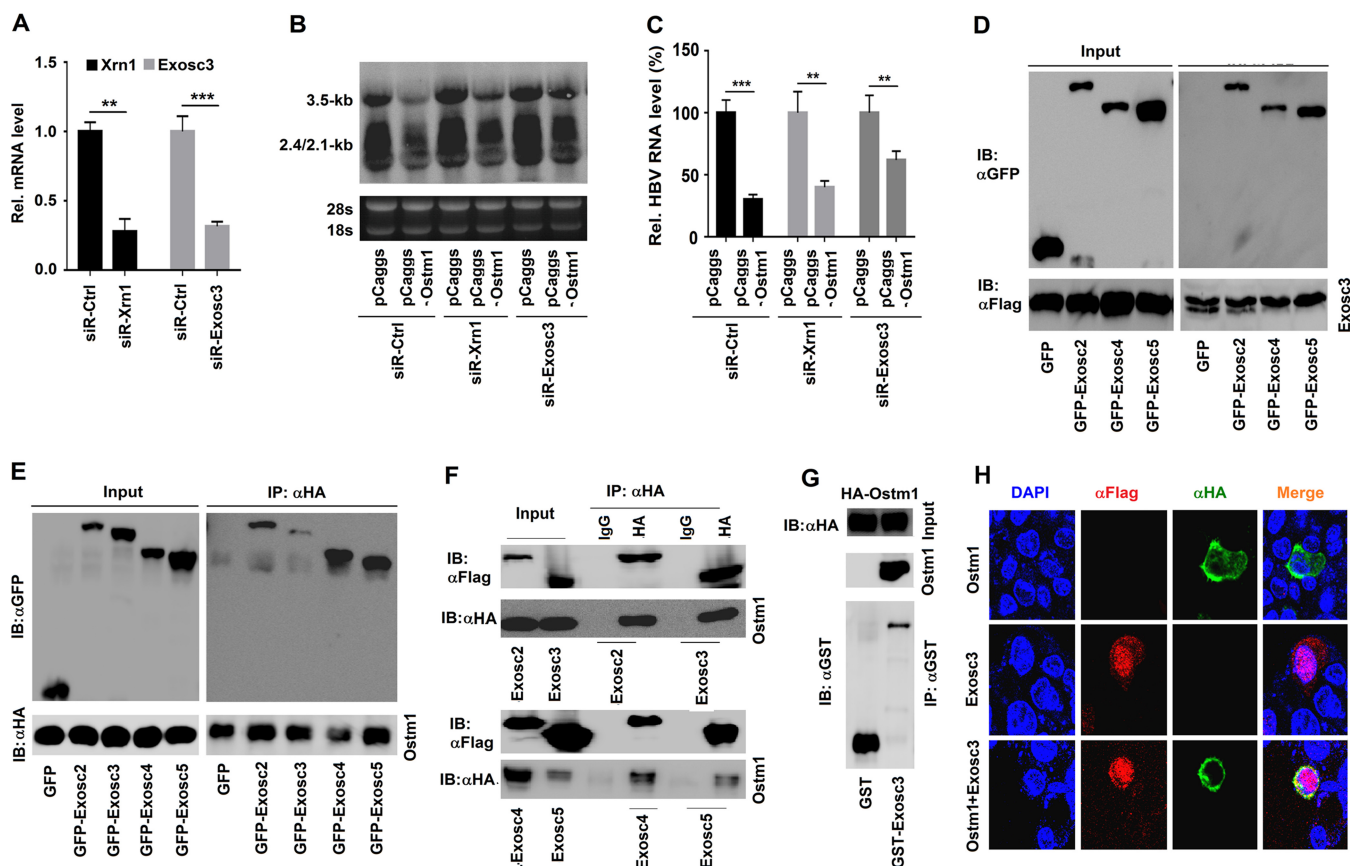


**FIG 6** The RNA exosome is involved in Ostm1-mediated degradation of HBV RNAs. (A to C) HepG2 cells were transfected with 100 nM siRNA targeting Xrn1 (siR-Xrn1), Exosc3 (siR-Exosc3), or the control (siR-Ctrl) together with pBlue-HBV 1.3 and pCaggs-Ostm1 for 48 h. (A) Xrn1 and Exosc3 mRNA were quantified using qRT-PCR, and (B) HBV RNAs were analyzed with Northern blot analysis. (C) The results of Northern blot analysis were quantified. (D) HEK293T cells were cotransfected Flag-Exosc3 with RNA exosome component proteins (pGFP-Exosc2, 4, and 5), and Crude extracts (input) were subjected to immunoprecipitation (IP) with Flag antibody. (E) HEK293T cells were cotransfected pCaggs-Ostm1 with RNA exosome component proteins (pGFP-Exosc2, 3, 4, and 5). HEK293T cells were collected, and crude extracts (input) were subjected to immunoprecipitation (IP) with HA antibody. Crude extracts and IP fractions were analyzed using Western blotting. (F) HEK293T cells were cotransfected with Ostm1 and RNA exosome component proteins (Flag-Exosc2, 3, 4, and 5), and IP of cell extracts was performed using anti-HA antibody. (G) Expressed and purified GST-Exosc3 or GST alone was incubated with GST-protein A/G beads. After incubation, the beads were incubated with HA-Ostm1 cell extracts. (H) HA-Ostm1 or Flag-Exosc3 was singly transfected in HepG2 cells for 48 h or was concomitantly transfected in HepG2 cells for 48 h. The cells were fixed and immunostained with anti-HA and anti-Flag antibody. After the nucleus was stained by DAPI (4'-diamidino-2-phenylindole), the locations of Ostm1 and Exosc3 were analyzed with immunofluorescence staining. \*,  $P < 0.05$ ; \*\*,  $P < 0.01$ ; \*\*\*,  $P < 0.001$ .

Ostm1- $\Delta$ R, whereas they were not affected by Ostm1- $\Delta$ C, Ostm1- $\Delta$ Tm, Ostm1- $\Delta$ Tm+ $\Delta$ C, or Ostm1- $\Delta$ N (Fig. 7D). Immunoblot analysis revealed that Ostm1, Ostm1- $\Delta$ C, Ostm1- $\Delta$ Tm, Ostm1- $\Delta$ Tm+ $\Delta$ C, Ostm1- $\Delta$ N, and Ostm1- $\Delta$ R were clearly detected in cell extracts; only Ostm1- $\Delta$ Tm and Ostm1- $\Delta$ Tm+ $\Delta$ C were secreted into the medium (Fig. 7B). The result that Ostm1- $\Delta$ Tm+ $\Delta$ C was secreted into the medium is consistent with previous reports (10). Therefore, these results revealed that the N-terminal domain, the transmembrane (Tm) domain, and the C-terminal domain of Ostm1 are required for Ostm1-mediated repression of HBV replication. Moreover, HEK293T cells were cotransfected with Flag-Exosc3 and different truncated Ostm1 mutants. Co-IP analysis revealed that Ostm1, Ostm1- $\Delta$ Tm, Ostm1- $\Delta$ N, and Ostm1-R could interact with Exosc3, whereas Ostm1- $\Delta$ C and Ostm1- $\Delta$ Tm+ $\Delta$ C failed to interact with Exosc3, revealing that the C-terminal domain of Ostm1 is involved in the interaction of Ostm1 with Exosc3 (Fig. 7E). Furthermore, we studied the intracellular localization of the truncated Ostm1 proteins. Laser scanning confocal microscopy showed that Ostm1, Ostm1- $\Delta$ C, Ostm1- $\Delta$ Tm, Ostm1- $\Delta$ Tm+ $\Delta$ C, and Ostm1- $\Delta$ R mainly localized in the cytoplasm, while Ostm1- $\Delta$ N distributed in both the cytoplasm and nuclei (Fig. 7F). Taken together, these results suggested that Ostm1 relies on Tm and the N-terminal domain to locate to the intracellular vesicles (mainly endoplasmic reticulum, endosomes, and lysosomes) in the

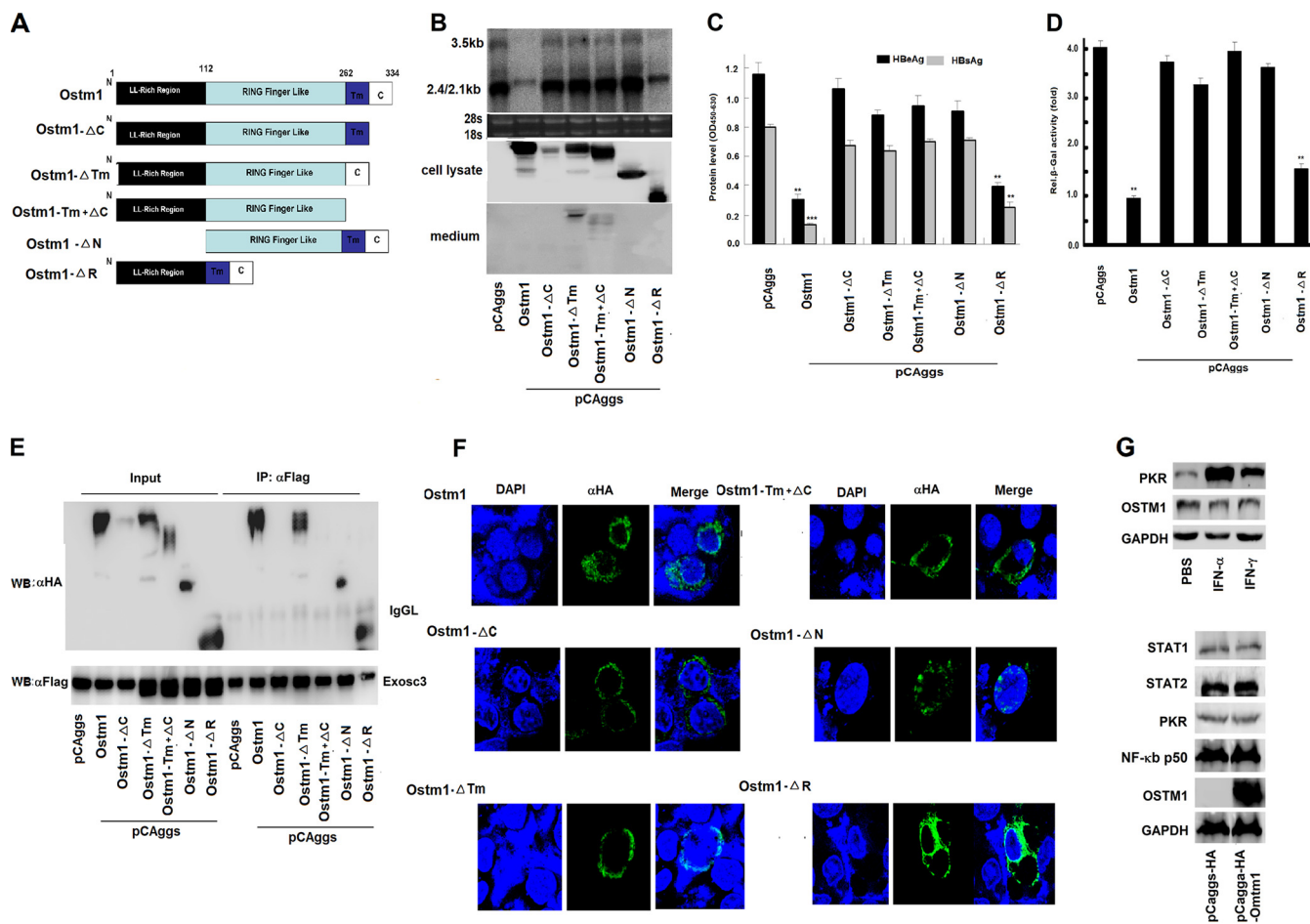


**FIG 7** Ostm1 represses HBV replication via N-terminal domain and C-terminal domain independent of the IFN signaling pathway. (A) Schematic diagrams of structures of Ostm1 protein and its mutants. (B to D) HepG2 cells were cotransfected with pBlue-HBV 1.3 or β-gal-HBV and different Ostm1 mutants for 48 h. (B) The levels of HBV RNAs were analyzed with Northern blotting. (C) Secreted HBsAg and HBeAg in cell culture supernatants were detected using ELISA. (D) The β-gal activity of pCDNA3.1-CMV-β-gal-HBV was then assessed. (E) HEK293T cells were cotransfected with Flag-Exosc3 and different mutants of Ostm1, and IP of cell extracts was performed by using anti-Flag antibody. (F) Ostm1 and different Ostm1 mutants were transfected in HepG2 cells for 48 h. The cells were fixed and immunostained with anti-HA antibody. After the nucleus was stained by DAPI (4′6-diamidino-2-phenylindole), the locations of proteins were analyzed with immunofluorescence staining. (G) HepG2 cells were treated with exogenous IFN-α and IFN-γ (600 U/ml) for 24 h before cells were harvested. The expression of Ostm1 was determined using Western blotting. (H) HepG2 cells were transfected with Ostm1 and control vector for 48 h. IFN downstream proteins (STAT1, STAT2, p50, and PKR) were checked with Western blotting. \*,  $P < 0.05$ ; \*\*,  $P < 0.01$ ; \*\*\*,  $P < 0.001$ .

cytoplasm and depends on the C-terminal domain to recruit the RNA exosome complex to HBV transcripts and degrade HBV RNAs.

CHB is associated with inflammatory cytokine production upon the activation of host innate immunity, and the dynamic balance between immune responses and virus replication determine the disease progression (27). IFN-induced intrahepatic genes play indispensable roles in controlling HBV replication (28, 29). Here, we investigated the correlation between Ostm1 and the IFN pathway. The effect of IFNs on the expression of Ostm1 was evaluated for HepG2 cells treated with IFN-α or IFN-γ. Double-stranded RNA activated protein kinase (PKR), which is one of several enzymes induced by interferon and a key molecule mediating the antiviral effect of interferon, was significantly induced by IFN-α and IFN-γ, whereas Ostm1 was not affected by IFN-α or IFN-γ (Fig. 7G), suggesting that Ostm1 production is not regulated by IFNs. The role of Ostm1 in the regulation of the IFN pathway was also determined in HepG2 cells transfected with pCaggs-HA or pCaggs-HA-Ostm1. Notably, the components of the IFN signaling pathway, including the signal transducer and activator of transcription 1 (STAT1), STAT2, PKR, and nuclear factor kappa B subunit p50 (NF-κB p50), were not affected by Ostm1 (Fig. 7H), indicating that Ostm1 is not involved in the regulation of the IFN

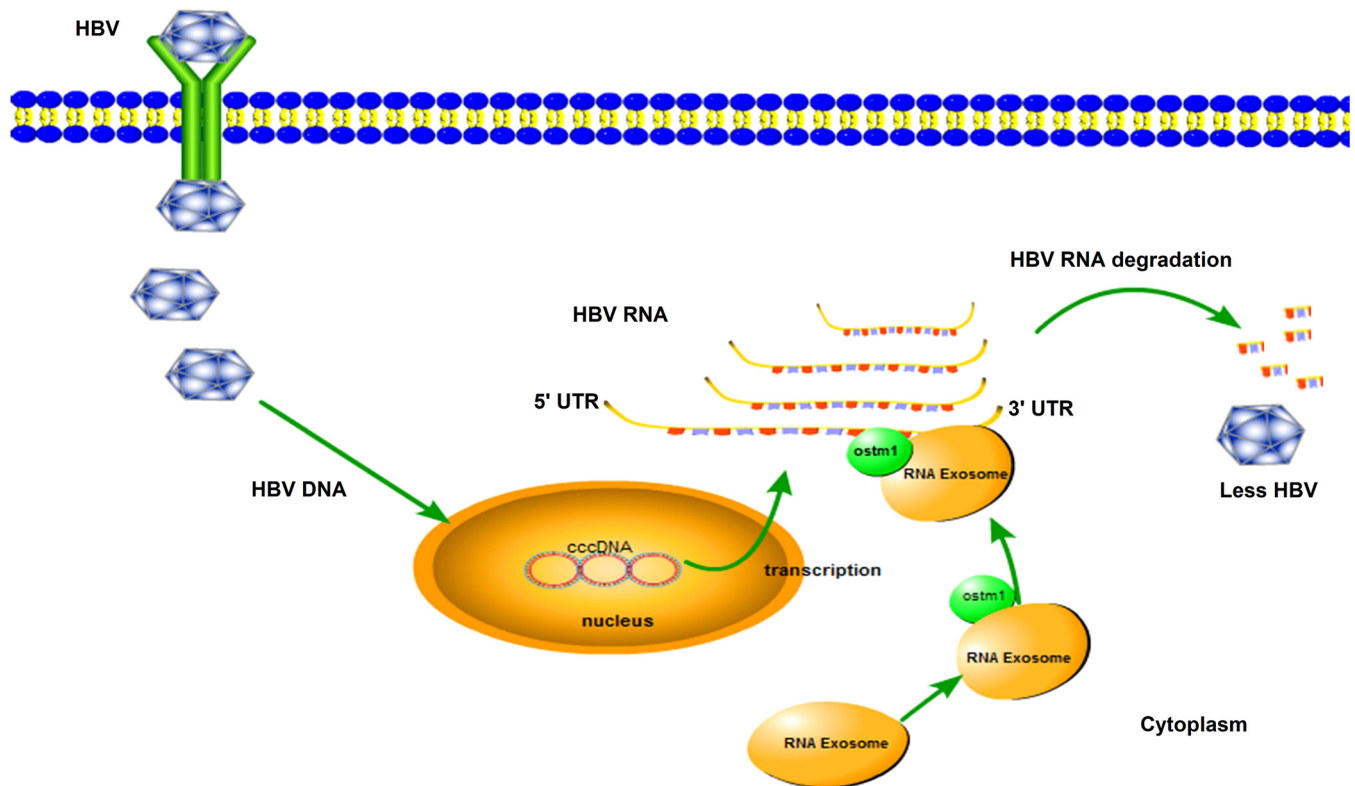


**FIG 8** Proposed mechanism underlying Ostm1-mediated inhibition of HBV replication. HBV virions enter the cell dependent on the sodium taurocholate cotransporting polypeptide (NTCP) receptor. In the nucleus, HBV rcDNA forms cccDNA, and cccDNA serves as the template to produce HBV mRNAs (pgRNA, 2.4/2.1-kb RNA, and 0.7-kb RNA) encoding surface antigens, core, HBeAg, HBx, and DNA polymerase. The pgRNA is encapsidated, together with polymerase, and reverse transcribed into (–) DNA (negative-strand DNA) inside the nucleocapsid. (+) DNA (positive-strand DNA) synthesis from (–) DNA generates rcDNA and forms HBV virions, which are released from the cells. The RNA degradation pathways (3′-5′ decay and 5′-3′ decay) can degrade aberrant mRNA and viral RNA. Ostm1 can interact with the RNA exosome and recruit it to HBV mRNAs, degrading HBV mRNAs and resulting in less HBV.

pathway. These results suggested that the anti-HBV activity of Ostm1 is independent of IFN signaling. Taken together, these findings revealed a distinct mechanism by which Ostm1 recruits the RNA exosome to restrict HBV replication (Fig. 8).

## DISCUSSION

Many cell factors can regulate HBV mRNA at the transcription and posttranscription levels. HNF1 $\alpha$  activates the EnhII/core promoter to promote HBV replication (30). HNF4 $\alpha$  enhances the EnhII/core, SP1, and SP2 promoters to support HBV replication (31). Sirt1 represses the EnhII/core promoter to inhibit HBV replication (32). La protein contributes to HBV pregenomic RNA stability (33), but ZAP, MyD88, AID, Prdx1, HNF6, and ISG20 reduce HBV pregenomic RNA stability (19–22, 34, 35). In this study, we revealed that Ostm1 attenuates the levels of HBV secreted proteins, RNA transcripts, and DNA. Ostm1 overexpression reduces, whereas Ostm1 suppression enhances, the levels of HBV transcripts and proteins in hepatoma cells and NTCP-HepG2 cells. Detailed studies unexpectedly demonstrated that Ostm1-mediated HBV RNA inhibition is independent of HBV intrinsic promoters and thus suggested that Ostm1 downregulates HBV replication primarily through posttranscriptional regulation or RNA stability. We further identified that Ostm1 promotes HBV pgRNA degradation, and Ostm1-mediated HBV RNA inhibition exclusively occurs in the cytoplasm. Thus, Ostm1 accelerates the decay of HBV pregenomic RNA in the cytoplasm.

Like transcription and translation, mRNA decay is a tightly controlled process that is determined by *cis*-acting elements within the mRNA and *trans*-acting factors. Notably, all HBV transcripts contain most of the *cis*-acting posttranscriptional regulatory elements (PRE) (nucleotides 1151 to 1805), including 3 conserved RNA structures—stem

loop  $\alpha$  (SL $\alpha$ ; nucleotides 1292 to 1321) and SL $\beta$  (nucleotides 1417 to 1458) of the PRE at the 3' end and the epsilon element ( $\epsilon$ ) at the 3' end or both ends. The  $\epsilon$  element located at the 5' end of the pgRNA is necessary for viral replication and packaging (36, 37). The HBV PRE is proposed to contain binding sites for cellular proteins which mediate function and can enhance the expression of HBV transcripts and the nuclear export of unspliced HBV subgenomic RNAs. In contrast, the PRE is not involved in the nuclear export of the full-length pgRNA (36, 38, 39). La binds to HBV RNAs to protect them from endonuclease cleavage (40). ZAP, AID, MyD88, Prdx1, HNF6, and ISG20 promote HBV RNA decay through a process that requires a specific region of HBV RNAs and RNA decay machines (19–22, 34, 35). La contributes to HBV pregenomic RNA stability through specific binding to HBV RNA (1270 to 1295) (33). ZAP binds to the ZAP-responsive element in HBV (1820 to 1918) and recruits the RNA exosome, resulting in HBV RNA degradation (20). The RNA sequence of the HBV (1804 to 2454) region is a crucial *cis*-regulatory sequence for MyD88-induced decay of HBV RNAs (19). ISG20 inhibits HBV replication through direct binding to the epsilon ( $\epsilon$ ) stem-loop structure of viral RNA (35). Here, we identified that the HBV (837 to 1065 and 1598 to 1796), regions, which are common sequences for pgRNA, 2.4-kb mRNA, and 2.1-kb mRNA, are crucial *cis*-regulatory sequences for Ostm1-induced HBV RNA decay. Obviously, the response regions of HBV RNA for Ostm1-induced HBV RNA decay are different from those of La, ZAP, ISG20, and MyD88, but the region HBV (1598 to 1796), located at the 3' end of the PRE, is not classical SL $\alpha$  or SL $\beta$ . Thus, there exists an unknown element that can bind Ostm1 protein in the 3' end of the PRE (1151 to 1805).

Through targeting of viral RNA for clearance, the host RNA exosome has been implicated in the host defense against viral infection (12). The RNA exosome complex consists of the core components and cofactors. The cofactors of the RNA exosome are responsible for specifically binding to substrate mRNA (15). We determined that Ostm1 interacts with the RNA exosome complex, and blemishing the function of the RNA exosome by knocking down Exosc3 seriously weakened Ostm1-mediated HBV RNA inhibition. We also revealed that HBV transcripts could form a specific complex with Ostm1. Taken together, this evidence suggested that Ostm1 recruits RNA exosomes to HBV RNAs, thereby downregulating HBV transcripts.

Ostm1 interacts with CIC-7 and RGS-GAIP through the N-terminal domain, depending on the RING finger-like cytoplasmic domain to degrade *G $\alpha$ i3* (6, 7). The C-terminal domain is required for Ostm1 interacting with kinesin 5B (10). Using serial deletion mutants of Ostm1, we identified that the N-terminal domain and C-terminal domain (a transmembrane domain and a short C terminus) are critical for the inhibitory effects on HBV RNAs, whereas the RING finger-like cytoplasmic domain is surplus for Ostm1-mediated inhibition of HBV RNAs. Previous reports showed that Ostm1 is a type I transmembrane protein that localizes to intracellular vesicles (mainly endoplasmic reticulum, endosomes, and lysosomes), that the Tm domain of Ostm1 has an important role in the localization of Ostm1 to intracellular vesicles (6, 8, 10), and that mRNAs are cotransported with membranous compartments such as the endoplasmic reticulum (ER) and endosomes (41). Thus, truncated Tm domain of Ostm1 cannot localize to intracellular vesicles and loses the function of promoting the decay of HBV RNAs. Laser scanning confocal microscopy showed that Ostm1- $\Delta$ N distributed in both the cytoplasm and nuclei, which is different from the location of Ostm1 only in the cytoplasm. Several proteins (e.g., myelin regulatory factor [MYRF] and a nonstructural protein of BAdV-3) have been reported to be transported to the nucleus, relying on the cleavage process (42, 43). There is a possibility that the N-terminal domain of ostm1 blocks the translocation of ostm1 to the nuclei. Considering that ostm1 can interact with CIC-7 or RGS-GAIP depending on the N-terminal domain, Ostm1 might rely on the domain to interact with specific proteins which have close relationships with HBV RNAs. In addition, we proved that the C-terminal domain is required for Ostm1 to interact with Exosc3. It was reported that Ostm1 locates to intracellular vesicles (mainly endoplasmic reticulum, endosomes, and lysosomes), that the N-terminal region of Ostm1 is likely luminal, and that the C terminus of the protein is free in cytoplasm (6, 10). In the study,

we found Ostm1 can interact with RNA exosomes through the C-terminal region of Ostm1 and recruit RNA exosomes to intracellular vesicles, which are the mRNA enrichment region. The relationship between Ostm1 and the RNA exosome provides a rationale for the RNA exosome to degrade HBV RNAs. The IFN signaling pathway plays an important role in inhibiting HBV infection. The anti-HBV proteins (ZAP, MyD88, AID, and ISG20) have close relationships with IFNs or TNF- $\beta$  (19–21, 35). In the study, we found that Ostm1 has no relationship with the IFN pathway. IFN- $\alpha$  and IFN- $\gamma$  do not affect the expression of Ostm1, and Ostm1 cannot influence the expression of IFN downstream genes. Thus, Ostm1 may be an exceptional anti-HBV protein independent of IFN signaling.

Based on the data presented in this study, we propose the following model for the Ostm1-mediated inhibition of HBV replication. Ostm1 accelerates the degradation of HBV RNAs in the cytoplasm through a process that depends on HBV (837 to 1065 and 1598 to 1796) and recruits the RNA exosome complex. Thus, the antiviral function of Ostm1 may ultimately lead to the development of new therapeutics for HBV infection.

## MATERIALS AND METHODS

**Cell cultures and transfection.** Human hepatoma HepG2 cells, Huh7 cells, and HepG2.2.15 (derived from HepG2) cells, as well as human embryonic kidney (293T) cells and HeLa cells, were maintained in Dulbecco's modified Eagle medium (DMEM) (Gibco, Grand Island, NY, USA) supplemented with 10% fetal bovine serum (FBS), 100 U/ml penicillin, and 100  $\mu$ g/ml streptomycin. Cells were transfected with Lipofectamine 2000 (Invitrogen, IL, USA) or Neofect (Neofect Biotech, Beijing, China) according to the manufacturer's instructions.

**Analysis of secreted HBV antigens.** Cell culture supernatants were collected to measure the HBsAg and HBeAg concentrations using a commercial enzyme-linked immunosorbent assay (ELISA) kit (Kehua Bio-Engineering, Shanghai, China) according to the manufacturer's protocol.

**Plasmids, small interfering RNAs, antibodies, and reagents.** HBV-1.3 was generated from HepG2.2.15 cells (genotype D, subtype ayw, GenBank accession no. [U95551](#)) and inserted into pBlue-script II (Invitrogen). Plasmids pSV40/CMV-pgRNA, 2.4-kb, 2.1-kb, pTRE2-HBV, pCDNA-3.1-CMV- $\beta$ -gal-HBV, and pCaggs-HA-La were generous gifts from Deyin Guo (Wuhan University, China). The luciferase HBV promoter reporters were kindly provided by Ying Zhu (Wuhan University, China). The cDNA fragments of HBV pregenomic RNA from pBlue-HBV1.3 were inserted into pCDNA-3.1-CMV- $\beta$ -gal at the 3' end of the  $\beta$ -gal coding sequence. The sequence of HBV (with the deletion of nucleotides [nt] 837 to 1065 or 1598 to 1796) was inserted into pCDNA-3.1-CMV and generated pCMV-HBV( $\Delta$ M1), pCMV-HBV( $\Delta$ M2), and pCMV-HBV( $\Delta$ M1+ $\Delta$ M2). Ostm1, Exosc2, Exosc3, Exosc4, and Exosc5 cDNA were generously provided by Jiahui Han of Xiamen University and were separately constructed in pCaggs-HA and pEGFP-N1 to generate pHA-Ostm1, pEGFP-N1-Exosc2, pEGFP-N1-Exosc3, pEGFP-N1-Exosc4, and pEGFP-N1-Exosc5. Ostm1-C, Ostm1- $\Delta$ Tm, Ostm1- $\Delta$ Tm+ $\Delta$ C, Ostm1- $\Delta$ R, and Ostm1- $\Delta$ N were also subcloned into the pCaggs-HA. The Exosc2, Exosc3, Exosc4, and Exosc5 coding sequences were also constructed in pCDNA3.1-3 $\times$ Flag, containing an N-terminal 3 $\times$ Flag tag.

Specific siRNAs were purchased from Guangzhou RiboBio, and the sequences of the siRNA against Ostm1, Xrn1, and Exosc3 were reported previously (8, 21, 44). Oligonucleotides targeting Ostm1 were cloned into pLKO.1.

Antibodies against GAPDH, LaminA, GFP, GST, and Ostm1 were purchased from the ProteinTech Group (Wuhan, Hubei, China). Antibodies against Flag, hemagglutinin (HA), PKR, P50, STAT1, and STAT2 were purchased from Sigma-Aldrich (St. Louis, MO, USA). IFN- $\alpha$  was purchased from SanSheng Biotech (Shenyang, China). IFN- $\gamma$  was purchased from PeproTech, Inc. (New Jersey, USA).

**RNA immunoprecipitation.** RNA immunoprecipitation was conducted according to the protocol described in reference 45. Briefly, cells were lysed with polysome lysis buffer (100 mM KCl, 5 mM MgCl<sub>2</sub>, 10 mM HEPESPH, pH 7.0, 0.5% NP-40, 1 mM DTT, 400  $\mu$ M VRC, 100 U/ml RNase inhibitor, and protease inhibitor). Immunoprecipitation was performed with protein G-agarose beads (GE Healthcare) for 4 h at 4°C using anti-HA or IgG antibodies. Protein G was washed five times with cooled NT2 buffer (50 mM Tris-HCl, pH 7.4, 150 mM NaCl, 1 mM MgCl<sub>2</sub>, and 0.05% NP-40). The beads were resuspended in 100  $\mu$ l of NT2 buffer. The immunoprecipitated RNA was repurified with TRIzol reagent (Invitrogen, Carlsbad, CA) according to the manufacturer's instructions. The obtained RNAs and proteins were analyzed using RT-PCR and immunoblotting, respectively.

**Coimmunoprecipitation and GST pulldown assay.** The transfected cells ( $2 \times 10^6$  cells) were lysed in 500  $\mu$ l lysis buffer (250 mM Tris-HCl, pH 7.4, 150 mM NaCl, 1 mM EDTA, 1% NP-40, and 5% glycerol). Cell lysates were precleared using protein G-agarose beads (GE Healthcare) for 1 h at 4°C, mixed with the specific antibodies or IgG, and rocked overnight at 4°C. Beads were washed five times with washing buffer, resuspended and denatured in PBS with SDS-PAGE loading buffer, and separated by SDS-PAGE with subsequent immunoblot analysis.

Glutathione S-transferase (GST) protein and GST-Exosc3 protein were expressed by the *E. coli* BL21 strain and purified GST and GST-Exosc3 were incubated with glutathione Sepharose beads (GE Healthcare). Immobilized beads were washed 5 times with ice-cold PBS. The beads were incubated with extracts of cells of transfected Ostm1 plasmid overnight at 4°C. Then the beads were washed with PBS-Triton

X-100 buffer 5 times, and proteins were eluted in SDS loading buffer and analyzed using SDS-PAGE and immunoblotting.

**Luciferase assay.** HepG2 cells were cotransfected with reporter plasmids and their corresponding expression plasmids. At 48 h posttransfection, the cells were lysed and subjected to luciferase or  $\beta$ -galactosidase activity assays according to the manufacturer's instructions (Promega, Madison, WI).

**Northern blot analysis and HBV DNA analysis.** Total RNA was isolated using an Ultrapure RNA kit (CWBio, Beijing, China) assay according to the manufacturer's instructions. Ten micrograms of total RNA was separated in a 1.2% formaldehyde-agarose gel containing MOPS (morpholinepropanesulfonic acid) buffer and transferred onto a positively charged nylon membrane (GE Healthcare, Waukesha, WI). To detect HBV transcripts, the membrane was probed with a digoxigenin (DIG)-labeled specific RNA probe corresponding to nt 156 to 1061 of the HBV genome. The membranes were detected with the DIG Northern starter kit (Roche Diagnostics, Indianapolis, IN) according to the manufacturer's instructions. The numbers of 28S and 18S rRNAs were used as loading controls.

At 96 h posttransfection, the cells were washed with cold PBS and lysed in lysis buffer (50 mM Tris-HCl, pH 7.0, and 0.5% NP-40) at 4°C. Following centrifugation (100,000  $\times$  *g* for 5 min), the supernatants were digested with DNase (Promega, Madison, WI) at 37°C for 1 h, and then the enzymes were inactivated at 70°C for 15 min in the presence of 10 mM EDTA. The core-associated DNA was isolated using proteinase K digestion, phenol-chloroform extraction, and ethanol precipitation. HBV DNA was subjected to TaqMan real-time PCR in a Light Cycler instrument (Roche) using PCR primers (5'-AGAAACAACACATAGCGCCTCAT-3' and 5'-TGCCCTGCTGTAGATCTTG-3') and probe (5'-TGTGGGTCACCATATTCTTGGG-3').

**Quantitative RT-PCR analysis.** Total RNA was extracted with an Ultrapure RNA kit (CWBio, Beijing, China) according to the manufacturer's instructions. Total RNAs were reverse transcribed with oligo (DT). Real-time PCR was performed with a Light Cycler 480 instrument (Roche), and glyceraldehyde-3-phosphate dehydrogenase (GAPDH) was used as an internal control. The following primers were used: GAPDH forward primer: 5'-GGAAGGTGGGTCGGAGTCAACGG-3', GAPDH reverse primer: 5'-CTCGCTCCTGAAGATGGTGATGGG-3'; HBV 3.5-kb forward primer: 5'-GAGTGTGGATTCCGACTCC-3', HBV 3.5-kb reverse primer: 5'-GAGCGAGGGAGTCTTCT-3'; Ostm1 forward primer: 5'-ACTTCAACTGTTCCAGTCCCTTGC-3', Ostm1 reverse primer: 5'-TGGCAGAATGAGTTTGCCTT-3'; Xrn1 forward primer: 5'-AGTGGGCACCTCACTACC-3', Xrn1 reverse primer: 5'-TGCGCACCTGC TGCTTCA-3'; Exosc3 forward primer: 5'-GCCAGCTTCTTGTCTTAC-3', Exosc3 reverse primer: 5'-TTTT CCCACTTCTGTATG-3'.

**Viruses and infection.** For HBV infection, the HBV inoculum was concentrated 100-fold from the supernatants of HepaAD38 (provided by Ying Zhu of Wuhan University, China) cells by ultracentrifugation at 100,000  $\times$  *g* for 5 h at 4°C. For infection, HepG2-NTCP cells (provided by Ying Zhu of Wuhan University, China) were seeded in collagen I-coated 24-well plates and inoculated overnight, and medium was replaced with protoplast maintenance medium (PMM) with 2% fetal bovine serum for 12 h. PMM was supplemented with transferrin, insulin, and sodium selenite (ITS), 10 ng/ml of human epidermal growth factor (EGF), 2 mM L-glutamine, 40 ng/ml of dexamethasone, 2% dimethyl sulfoxide (DMSO), 18  $\mu$ g/ml of hydrocortisone, 100 U/ml of penicillin, and 100 U/ml of streptomycin. Then, 1,000 genome equivalents (GEs) of HBV per cell were put in PMM containing 4% (wt/vol) polyethylene glycol 8000 (PEG 8000) for 16 h. Virus-containing medium was removed, and cells were washed five times and further incubated in PMM with 2% serum (30, 31).

**Cytoplasmic and nuclear RNA isolation.** Nucleoplasm separation of cells was conducted according to the protocol described in reference 46. Briefly, 48 h posttransfection, cells were harvested and lysed in lysis buffer (50 mM Tris-HCl, pH 8.0, 0.5% NP-40, 100 mM NaCl, 5 mM MgCl<sub>2</sub>, 1 U/ $\mu$ l RNasin, 1 mM dithiothreitol [DTT]) at 4°C at 12,000 rpm for 5 min. Then, the nuclei were precipitated by centrifugation at 12,000 rpm for 2 min. Cytoplasmic RNA in the supernatants and nuclear RNA from nuclear pellets were separately extracted using an Ultrapure RNA kit (CWBio, Beijing, China) and TRIzol reagent (Invitrogen, Carlsbad, CA) according to the manufacturer's instructions. The nuclear and cytoplasmic RNAs were then subjected to Northern blot analysis.

**Immunofluorescence and confocal analyses.** HepG2 cells were grown in glass-bottom dishes. Twenty-four hours after transfection, cells were fixed with 4% paraformaldehyde for 15 min, washed 3 times with PBS, permeabilized with PBS containing 0.2% Triton X-100 for 5 min, washed three times with PBS, and blocked with PBS containing 5% bovine serum albumin for 30 min at room temperature. The cells were then incubated with anti-HA and anti-Flag overnight at 4°C, followed by incubation with fluorescein isothiocyanate (FITC)-conjugated goat anti-mouse IgG and cy3-conjugated goat anti-rabbit IgG for 45 min at room temperature, and were then stained with DAPI (4', 6'-diamidino-2-phenylindole). Cells were viewed using confocal laser microscopy (FluoView Fv1000; Olympus).

**Statistical analysis.** Statistical analysis was performed with GraphPad Prism 5. Individual experiments were conducted in triplicate, and repetitive assays with similar results were performed to confirm the reproducibility of the result. The results are presented as means  $\pm$  standard deviation (SD). Differences were considered statistically significant at a *P* value of  $\leq$ 0.05.

## ACKNOWLEDGMENTS

This work was supported by the National Natural Science Foundation of China (81730061 and 31800147), the National Health and Family Planning Commission of the People's Republic of China, the National Mega Project on Major Infectious Disease Prevention (2017ZX10103005 and 2017ZX10202201), and the Guangdong Province "Pearl River Talent Plan" Innovation and Entrepreneurship Team Project (2017ZT07Y580). The funders

had no role in study design, data collection and interpretation, or the decision to submit the work for publication.

We thank Jiahua Han of Xiamen University, China, for kindly providing the cDNA of Exosc2, Exosc3, Exosc4, Exosc5, and Exosc7, Ying Zhu of Wuhan University, China, for kindly providing HepG2-NTCP cells and HepaAD38 cells, and Deyin Guo of Wuhan University, China, for kindly providing the pSV40/CMV-pgRNA, 2.4-kb, 2.1-kb, pCMV- $\beta$ -gal-HBV, pCaggs-La, and pTRE2-HBV plasmids.

We declare that we have no conflicts of interest.

## REFERENCES

- Elgouhari HM, Abu-Rajab Tamimi TI, Carey WD. 2008. Hepatitis B virus infection: understanding its epidemiology, course, and diagnosis. *Cleve Clin J Med* 75:881–889. <https://doi.org/10.3949/cjcm.75a.07019>.
- Venkatakrishnan B, Zlotnick A. 2016. The structural biology of hepatitis B virus: form and function. *Annu Rev Virol* 3:429–451. <https://doi.org/10.1146/annurev-virology-110615-042238>.
- Chalhoub N, Benachenhou N, Rajapurohitam V, Pata M, Ferron M, Frattini A, Villa A, Vacher J. 2003. Grey-lethal mutation induces severe malignant autosomal recessive osteopetrosis in mouse and human. *Nat Med* 9:399–406. <https://doi.org/10.1038/nm842>.
- Pangrazio A, Poliani PL, Megarbane A, Lefranc G, Lanino E, Di Rocco M, Rucci F, Lucchini F, Ravanini M, Facchetti F, Abinun M, Vezzoni P, Villa A, Frattini A. 2006. Mutations in OSTM1 (grey lethal) define a particularly severe form of autosomal recessive osteopetrosis with neural involvement. *J Bone Miner Res* 21:1098–1105. <https://doi.org/10.1359/jbmr.060403>.
- Prinetti A, Rocchetta F, Costantino E, Frattini A, Caldana E, Rucci F, Bettiga A, Poliani PL, Chigorno V, Sonnino S. 2009. Brain lipid composition in grey-lethal mutant mouse characterized by severe malignant osteopetrosis. *Glycoconj J* 26:623–633. <https://doi.org/10.1007/s10719-008-9179-8>.
- Lange PF, Wartosch L, Jentsch TJ, Fuhrmann JC. 2006. CIC-7 requires Ostm1 as a beta-subunit to support bone resorption and lysosomal function. *Nature* 440:220–223. <https://doi.org/10.1038/nature04535>.
- Fischer T, De Vries L, Meerloo T, Farquhar MG. 2003. Promotion of G alpha i3 subunit down-regulation by GIPN, a putative E3 ubiquitin ligase that interacts with RGS-GAIP. *Proc Natl Acad Sci U S A* 100:8270–8275. <https://doi.org/10.1073/pnas.1432965100>.
- Feigin ME, Malbon CC. 2008. OSTM1 regulates beta-catenin/Lef1 interaction and is required for Wnt/beta-catenin signaling. *Cell Signal* 20: 949–957. <https://doi.org/10.1016/j.cellsig.2008.01.009>.
- Liu Y, Zhang ZC, Qian SW, Zhang YY, Huang HY, Tang Y, Guo L, Li X, Tang QQ. 2013. MicroRNA-140 promotes adipocyte lineage commitment of C3H10T1/2 pluripotent stem cells via targeting osteopetrosis-associated transmembrane protein 1. *J Biol Chem* 288:8222–8230. <https://doi.org/10.1074/jbc.M112.426163>.
- Pandruvada SN, Beaugregard J, Benjannet S, Pata M, Lazure C, Seidah NG, Vacher J. 2016. Role of Ostm1 cytosolic complex with kinesin 5B in intracellular dispersion and trafficking. *Mol Cell Biol* 36:507–521. <https://doi.org/10.1128/MCB.00656-15>.
- Garneau NL, Wilusz J, Wilusz CJ. 2007. The highways and byways of mRNA decay. *Nat Rev Mol Cell Biol* 8:113–126. <https://doi.org/10.1038/nrm2104>.
- Moon SL, Wilusz J. 2013. Cytoplasmic viruses: rage against the (cellular RNA decay) machine. *PLoS Pathog* 9:e1003762. <https://doi.org/10.1371/journal.ppat.1003762>.
- Schoenberg DR, Maquat LE. 2012. Regulation of cytoplasmic mRNA decay. *Nat Rev Genet* 13:246–259. <https://doi.org/10.1038/nrg3160>.
- Kilchert C, Wittmann S, Vasiljeva L. 2016. The regulation and functions of the nuclear RNA exosome complex. *Nat Rev Mol Cell Biol* 17:227–239. <https://doi.org/10.1038/nrm.2015.15>.
- Zinder JC, Lima CD. 2017. Targeting RNA for processing or destruction by the eukaryotic RNA exosome and its cofactors. *Genes Dev* 31:88–100. <https://doi.org/10.1101/gad.294769.116>.
- Staals RH, Bronkhorst AW, Schilders G, Slomovic S, Schuster G, Heck AJ, Rajmakers R, Pruijn GJ. 2010. Dis3-like 1: a novel exoribonuclease associated with the human exosome. *EMBO J* 29:2358–2367. <https://doi.org/10.1038/emboj.2010.122>.
- Tomecki R, Kristiansen MS, Lykke-Andersen S, Chlebowski A, Larsen KM, Szczesny RJ, Drazkowska K, Pastula A, Andersen JS, Stepien PP, Dziembowski A, Jensen TH. 2010. The human core exosome interacts with differentially localized processive RNases: hDIS3 and hDIS3L. *EMBO J* 29:2342–2357. <https://doi.org/10.1038/emboj.2010.121>.
- Burkard KT, Butler JS. 2000. A nuclear 3'-5' exonuclease involved in mRNA degradation interacts with poly(A) polymerase and the hnRNA protein Npl3p. *Mol Cell Biol* 20:604–616. <https://doi.org/10.1128/mcb.20.2.604-616.2000>.
- Li J, Lin S, Chen Q, Peng L, Zhai J, Liu Y, Yuan Z. 2010. Inhibition of hepatitis B virus replication by MyD88 involves accelerated degradation of pregenomic RNA and nuclear retention of pre-S/S RNAs. *J Virol* 84:6387–6399. <https://doi.org/10.1128/JVI.00236-10>.
- Mao R, Nie H, Cai D, Zhang J, Liu H, Yan R, Cuconati A, Block TM, Guo JT, Guo H. 2013. Inhibition of hepatitis B virus replication by the host zinc finger antiviral protein. *PLoS Pathog* 9:e1003494. <https://doi.org/10.1371/journal.ppat.1003494>.
- Liang G, Liu G, Kitamura K, Wang Z, Chowdhury S, Monjurul AM, Wakae K, Koura M, Shimada M, Kinoshita K, Muramatsu M. 2015. TGF-beta suppression of HBV RNA through AID-dependent recruitment of an RNA exosome complex. *PLoS Pathog* 11:e1004780. <https://doi.org/10.1371/journal.ppat.1004780>.
- Deng L, Gan X, Ito M, Chen M, Aly HH, Matsui C, Abe T, Watashi K, Wakita T, Suzuki T, Okamoto T, Matsuura Y, Mizokami M, Shoji I, Hotta H. 2018. Peroxiredoxin 1, a novel HBx-interacting protein, interacts with exosome component 5 and negatively regulates hepatitis B virus (HBV) propagation through degradation of HBV RNA. *J Virol* 93:e02203–18. <https://doi.org/10.1128/JVI.02203-18>.
- Aly HH, Suzuki J, Watashi K, Chayama K, Hoshino S, Hijikata M, Kato T, Wakita T. 2016. RNA exosome complex regulates stability of the hepatitis B virus X-mRNA transcript in a non-stop-mediated (NSD) RNA quality control mechanism. *J Biol Chem* 291:15958–15974. <https://doi.org/10.1074/jbc.M116.724641>.
- Yan H, Zhong G, Xu G, He W, Jing Z, Gao Z, Huang Y, Qi Y, Peng B, Wang H, Fu L, Song M, Chen P, Gao W, Ren B, Sun Y, Cai T, Feng X, Sui J, Li W. 2012. Sodium taurocholate cotransporting polypeptide is a functional receptor for human hepatitis B and D virus. *Elife* 1:e00049. <https://doi.org/10.7554/eLife.00049>.
- Yan H, Peng B, Liu Y, Xu G, He W, Ren B, Jing Z, Sui J, Li W. 2014. Viral entry of hepatitis B and D viruses and bile salts transportation share common molecular determinants on sodium taurocholate cotransporting polypeptide. *J Virol* 88:3273–3284. <https://doi.org/10.1128/JVI.03478-13>.
- Preker P, Nielsen J, Kammler S, Lykke-Andersen S, Christensen MS, Mapendano CK, Schierup MH, Jensen TH. 2008. RNA exosome depletion reveals transcription upstream of active human promoters. *Science* 322:1851–1854. <https://doi.org/10.1126/science.1164096>.
- Guidotti LG, Chisari FV. 2006. Immunobiology and pathogenesis of viral hepatitis. *Annu Rev Pathol* 1:23–61. <https://doi.org/10.1146/annurev.pathol.1.110304.100230>.
- Wieland S, Thimme R, Purcell RH, Chisari FV. 2004. Genomic analysis of the host response to hepatitis B virus infection. *Proc Natl Acad Sci U S A* 101:6669–6674. <https://doi.org/10.1073/pnas.0401771101>.
- Wieland SF, Vega RG, Müller R, Evans CF, Hilbush B, Guidotti LG, Sutcliffe JG, Schultz PG, Chisari FV. 2003. Searching for interferon-induced genes that inhibit hepatitis B virus replication in transgenic mouse hepatocytes. *J Virol* 77:1227–1236. <https://doi.org/10.1128/jvi.77.2.1227-1236.2003>.
- Wang WX, Li M, Wu X, Wang Y, Li ZP. 1998. HNF1 is critical for the

- liver-specific function of HBV enhancer II. *Res Virol* 149:99–108. [https://doi.org/10.1016/s0923-2516\(98\)80085-x](https://doi.org/10.1016/s0923-2516(98)80085-x).
31. Tang H, McLachlan A. 2001. Transcriptional regulation of hepatitis B virus by nuclear hormone receptors is a critical determinant of viral tropism. *Proc Natl Acad Sci U S A* 98:1841–1846. <https://doi.org/10.1073/pnas.041479698>.
  32. Ren JH, Tao Y, Zhang ZZ, Chen WX, Cai XF, Chen K, Ko BC, Song CL, Ran LK, Li WY, Huang AL, Chen J. 2014. Sirtuin 1 regulates hepatitis B virus transcription and replication by targeting transcription factor AP-1. *J Virol* 88:2442–2451. <https://doi.org/10.1128/JVI.02861-13>.
  33. Horke S, Reumann K, Rang A, Heise T. 2002. Molecular characterization of the human La protein-hepatitis B virus RNA.B interaction in vitro. *J Biol Chem* 277:34949–34958. <https://doi.org/10.1074/jbc.M201911200>.
  34. Hao R, He J, Liu X, Gao G, Liu D, Cui L, Yu G, Yu W, Chen Y, Guo D. 2015. Inhibition of hepatitis B virus gene expression and replication by hepatocyte nuclear factor 6. *J Virol* 89:4345–4355. <https://doi.org/10.1128/JVI.03094-14>.
  35. Liu Y, Nie H, Mao R, Mitra B, Cai D, Yan R, Guo JT, Block TM, Mechti N, Guo H. 2017. Interferon-inducible ribonuclease ISG20 inhibits hepatitis B virus replication through directly binding to the epsilon stem-loop structure of viral RNA. *PLoS Pathog* 13:e1006296. <https://doi.org/10.1371/journal.ppat.1006296>.
  36. Smith GJ, 3rd, Donello JE, Lück R, Steger G, Hope TJ. 1998. The hepatitis B virus post-transcriptional regulatory element contains two conserved RNA stem-loops which are required for function. *Nucleic Acids Res* 26:4818–4827. <https://doi.org/10.1093/nar/26.21.4818>.
  37. Sommer G, Heise T. 2008. Posttranscriptional control of HBV gene expression. *Front Biosci* 13:5533–5547. <https://doi.org/10.2741/3097>.
  38. Lim CS, Brown CM. 2016. Hepatitis B virus nuclear export elements: RNA stem-loop alpha and beta, key parts of the HBV post-transcriptional regulatory element. *RNA Biol* 13:743–747. <https://doi.org/10.1080/15476286.2016.1166330>.
  39. Chen A, Panjaworayan TTN, Brown CM. 2014. Prospects for inhibiting the post-transcriptional regulation of gene expression in hepatitis B virus. *World J Gastroenterol* 20:7993–8004. <https://doi.org/10.3748/wjg.v20.i25.7993>.
  40. Ehlers I, Horke S, Reumann K, Rang A, Grosse F, Will H, Heise T. 2004. Functional characterization of the interaction between human La and hepatitis B virus RNA. *J Biol Chem* 279:43437–43447. <https://doi.org/10.1074/jbc.M402227200>.
  41. Jansen RP, Niessing D, Baumann S, Feldbrugge M. 2014. mRNA transport meets membrane traffic. *Trends Genet* 30:408–417. <https://doi.org/10.1016/j.tig.2014.07.002>.
  42. Meng J, Ma X, Tao H, Jin X, Witvliet D, Mitchell J, Zhu M, Dong MQ, Zhen M, Jin Y, Qi YB. 2017. Myrf ER-bound transcription factors drive *C. elegans* synaptic plasticity via cleavage-dependent nuclear translocation. *Dev Cell* 41:180–194. <https://doi.org/10.1016/j.devcel.2017.03.022>.
  43. Makadiya N, Gaba A, Tikoo SK. 2015. Cleavage of bovine adenovirus type 3 non-structural 100K protein by protease is required for nuclear localization in infected cells but is not essential for virus replication. *J Gen Virol* 96:2749–2763. <https://doi.org/10.1099/vir.0.000205>.
  44. Zhu Y, Chen G, Lv F, Wang X, Ji X, Xu Y, Sun J, Wu L, Zheng YT, Gao G. 2011. Zinc-finger antiviral protein inhibits HIV-1 infection by selectively targeting multiply spliced viral mRNAs for degradation. *Proc Natl Acad Sci U S A* 108:15834–15839. <https://doi.org/10.1073/pnas.1101676108>.
  45. Keene JD, Komisarow JM, Friedersdorf MB. 2006. RIP-Chip: the isolation and identification of mRNAs, microRNAs and protein components of ribonucleoprotein complexes from cell extracts. *Nat Protoc* 1:302–307. <https://doi.org/10.1038/nprot.2006.47>.
  46. Rio DC, Ares M, Jr, Hannon GJ, Nilsen TW. 2010. Preparation of cytoplasmic and nuclear RNA from tissue culture cells. *Cold Spring Harb Protoc* 2010:pdb.prot5441. <https://doi.org/10.1101/pdb.prot5441>.